Eur. Phys. J. D **23**, 359–368 (2003)
DOI: 10.1140/epjd/e2003-00062-4

THE EUROPEAN PHYSICAL JOURNAL D

Stability of charged metal clusters in the vicinity of an ionic charge

A classical investigation

K. Hamada[1,a], T. Wada[1], and C. Guet[2]

[1] Department of Physics, Konan University, 8-9-1 Okamoto, Higashinada, Kobe 658-8501, Japan
[2] Département de Physique Théorique et Appliquée, CEA-Ile de France, B.P. 12, 91680 Bruyères-le-Châtel, France

Received 5 November 2002 / Received in final form 27 January 2003
Published online 11 March 2003 –

Abstract. Stability of highly charged metal clusters in the electric field of an external ion is investigated with the classical liquid drop model. We study the optimum shape of the cluster which has a local minimum of the total energy, taking account of the effects of the surface charge polarization on the Coulomb energy and the cluster deformation on the surface energy. We find that the cluster deformation greatly affects the total energy of the system and that a cluster with a fissility larger than some critical value 0.7−0.8 can become unstable against deformation. We investigate the local competition between the Coulomb force and the surface tension at the cluster surface and show that the surface charge polarization which is induced by the external electric field significantly affects the shape of the cluster and its stability.

PACS. 36.40.Qv Stability and fragmentation of clusters – 36.40.Wa Charged clusters

1 Introduction

Stability of charged metal clusters and their fission have been investigated both experimentally [1–11] and theoretically [3,8,12–17]. Fission of metallic clusters is particularly interesting on account of the similarities and differences with the nuclear fission process [12].

Atomic nuclei and (charged) metal clusters can be expressed approximately as incompressible liquid drops due to their saturation properties. In nuclear physics, heavy elements, such as uranium, can be thermally activated by nuclear reactions, for example, by the absorption of a neutron. The nucleus deforms by the thermal fluctuation of the collective energy and the fission takes place [18,19]. The fission of atomic nuclei is observed only in heavy elements because the proton number of a nucleus is essentially proportional to its mass number. Also the mass number of a nucleus is limited to a value around 300 due to the decay by fission. Whereas, for metal clusters, the size and the charge can be chosen freely in principle. Hence, rich physical phenomena are expected for metal clusters.

Charged metal clusters are produced from neutral clusters either by laser ionization [1–6] or by ionization by collision with a beam of highly charged ions [7–11]. The latter method allows one to produce in peripheral collisions, highly charged metal clusters with low excitation energy, which is particularly suitable to investigate the instability induced by the Coulomb force.

In view of similarities between metal clusters and atomic nuclei, the classical liquid drop model used in nuclear physics has been applied to estimate the macroscopic energy of a charged metal cluster and its stability [12]. In this model, for atomic nuclei, the charges are uniformly distributed inside the droplet, whereas for multiply charged metal clusters, the charges exist only on the surface of the droplet and can be polarized. The polarization of the surface charge significantly affects the stability of highly charged metal clusters, because it leads to a lowering of the energy barriers against fission [12].

Stability of a charged droplet against any small deformation is determined by the competition between the repulsive Coulomb energy and the surface tension that tends to keep a spherical shape. Over a century ago, Lord Rayleigh [20] showed that for a spherical charged droplet, the fissility parameter X which provides a measure of stability, is defined as the ratio of the Coulomb energy to twice the surface energy, *i.e.* $X = E_c/2E_s$. For $X = 1$, any infinitesimal quadrupole deformation destabilizes the droplet, because there is no energy barrier for the breakup. For $X > 1$, higher order multipole infinitesimal deformations destabilize the droplet [12,20].

In numerical calculations with generalized Cassinian-oval parameterization, it was found that protrusions are developed at the tips of a droplet already for $X = 0.9$, which leads to a Rayleigh-Taylor instability [21].

[a] e-mail: hamada@konan-u.ac.jp

For spheroidal deformations of a charged droplet, Krappe [22] investigated analytically local stabilities. He compared the Coulomb force which destabilizes the spheroid with the surface tension which stabilizes it and showed that the local stability at the tip of the spheroid could be expressed in terms of a local fissility parameter associated with a sphere which would have the same size and charge. Setting the Coulomb force and the surface tension per unit area at the tip of the spheroid as P_c and P_s, respectively, one has $X = P_c/P_s$. He also discussed the effect of a homogeneous electric field along the symmetry axis on the stability of the spheroidal droplet and showed that the stability at the tip is expressed by an effective fissility that is the product of the fissility X and a coefficient (larger than one) depending on the strength of the electric field and the eccentricity of the spheroid.

In the present work, we consider a simple system composed of a charged sodium cluster Na_N^{Q+} with fissility X greater than 0.6 and a sodium ion Na_1^{1+}, which corresponds to the case that a charged metal cluster emits an ion or an ion passes near a charged metal cluster. We investigate the stability of the highly charged metal cluster in the external electric field of the ion with the classical liquid drop model, taking account of the effect of the surface charge polarization on the Coulomb energy and that of the cluster deformation on the surface energy. Since we calculate the static potential energy of the system, we suppose that the contribution of the rotation energy of the cluster to its deformation energy is small and that the relative motion of the system is slow enough for the cluster to take an equilibrium shape.

The present work is an extension of that discussed in reference [12]. In reference [12], they emphasize the importance of the effect of surface charge polarization on lowering the fission barriers for systems such that the saddle-point is characterized by two separated spherical fragments. In the present work, in addition to this effect, we include surface deformations which should be also important to estimate the stability of charged metal clusters more reliably.

In Section 2, we describe the procedure to calculate the total energy of the system. Results are given in Section 3 concerning the interaction energy, the shapes of the clusters, and the stability of the clusters. A summary is given in Section 4.

2 Energy calculation procedure

We describe here the procedure to calculate the total energy of a system made of a cluster and an ion within the classical liquid drop model. We assume that the two droplets (the cluster and the ion) are incompressible. To take account of the surface charge polarization, we suppose that the droplets are ideal conductors and the charges are distributed only on surfaces. We also introduce the cluster deformation so that the cluster has an optimal shape to minimize the total energy.

2.1 Liquid drop energy

In the liquid drop model, the energy of a droplet is given by the sum of the Coulomb energy E_c, the surface energy E_s, and the volume energy which is neglected here because we assume volume conservation. Hence the total energy is expressed as

$$E = E_c + E_s. \tag{1}$$

The surface energy is proportional to the total surface area $S = S_1 + S_2$ (the subscripts 1 and 2 are for the cluster and the ion, respectively)

$$E_s = \sigma S, \tag{2}$$

where σ ($0.20\,\mathrm{J/m^2}$ for sodium at melting point [12]) is the surface energy per unit area.

The Coulomb energy is expressed as a functional of the surface charge density ρ_1 and ρ_2 (in this paper, we use atomic units)

$$\begin{aligned} E_c[\rho_1,\rho_2] = {} & \frac{1}{2}\int_{S_1}\frac{\rho_1(\mathbf{r}_1)\rho_1(\mathbf{r}'_1)}{|\mathbf{r}_1-\mathbf{r}'_1|}\mathrm{d}S_1\mathrm{d}S'_1 \\ & + \frac{1}{2}\int_{S_2}\frac{\rho_2(\mathbf{r}_2)\rho_2(\mathbf{r}'_2)}{|\mathbf{r}_2-\mathbf{r}'_2|}\mathrm{d}S_2\mathrm{d}S'_2 \\ & + \int_{S_1,S_2}\frac{\rho_1(\mathbf{r}_1)\rho_2(\mathbf{r}_2)}{|\mathbf{r}_1-\mathbf{r}_2|}\mathrm{d}S_1\mathrm{d}S_2, \end{aligned} \tag{3}$$

where the first term, the second term and the last term are the self energy of the cluster, that of the ion and the interaction energy between the cluster and the ion, respectively. ρ_1 and ρ_2 satisfy the charge conservation conditions

$$\int_{S_1}\rho_1(\mathbf{r}_1)\mathrm{d}S_1 = Z_1, \tag{4}$$

$$\int_{S_2}\rho_2(\mathbf{r}_2)\mathrm{d}S_2 = Z_2. \tag{5}$$

As we suppose that the two droplets are ideal conductors, the electrostatic potential has to be constant throughout each droplet. This is achieved by finding ρ_1 and ρ_2 which minimize equation (3) under the constraints of the charge conservation, equations (4, 5). It corresponds to finding a local minimum of the following functional

$$\begin{aligned} F[\rho_1,\rho_2] = E_c[\rho_1,\rho_2] & - \phi_1\int_{S_1}\rho_1(\mathbf{r}_1)\mathrm{d}S_1 \\ & - \phi_2\int_{S_2}\rho_2(\mathbf{r}_2)\mathrm{d}S_2, \end{aligned} \tag{6}$$

where ϕ_1 and ϕ_2 are Lagrange multipliers. Variation of equation (6) with respect to ρ_1 and ρ_2 independently gives

$$\phi_1 = \int_{S_1}\frac{\rho_1(\mathbf{r}'_1)}{|\mathbf{r}_1-\mathbf{r}'_1|}\mathrm{d}S'_1 + \int_{S_2}\frac{\rho_2(\mathbf{r}_2)}{|\mathbf{r}_1-\mathbf{r}_2|}\mathrm{d}S_2, \tag{7}$$

$$\phi_2 = \int_{S_2}\frac{\rho_2(\mathbf{r}'_2)}{|\mathbf{r}_2-\mathbf{r}'_2|}\mathrm{d}S'_2 + \int_{S_1}\frac{\rho_1(\mathbf{r}_1)}{|\mathbf{r}_1-\mathbf{r}_2|}\mathrm{d}S_1, \tag{8}$$

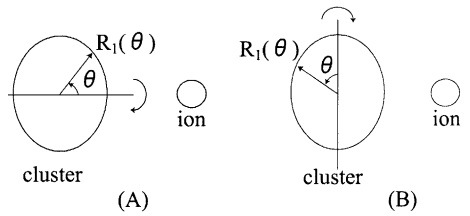

Fig. 1. Symmetry axis passing through the mass centers of the cluster and the ion, axis (A) (left); axis (B) that is perpendicular to axis (A) (right).

which are identical to the electrostatic potential of the cluster and the ion, respectively. Equations (7, 8) are solved numerically by using the method described in Appendix A of reference [23].

Using equations (4, 5, 7, 8) for equation (3), we obtain the Coulomb energy as

$$E_{\rm c} = \frac{1}{2} Z_1 \phi_1 + \frac{1}{2} Z_2 \phi_2. \tag{9}$$

2.2 Deformation

The cluster surface is expanded in Legendre polynomials, assuming the axial symmetry

$$R_1(\theta) = R_1^0 \left(1 + \sum_n \alpha_n P_n(\cos\theta) \right) / \lambda, \tag{10}$$

$$R_1^0 = r_{\rm ws} N_1^{1/3}, \tag{11}$$

where α_n, λ and θ are the expansion coefficient of nth order, the volume conservation factor and the polar angle between the radial direction and the symmetry axis, respectively. R_1^0 is the radius of the spherical cluster, where N_1 is the size of the cluster and $r_{\rm ws}$ (4.0 Å for sodium) is Wigner-Seitz radius. The ion is fixed to the spherical shape which has the radius $R_2^0 = r_{\rm ws} N_2^{1/3}$ with the size $N_2 = 1$.

As for the symmetry axis, we consider the following two cases. One is the axis passing through the mass centers of the cluster and the ion: axis (A). The other is the axis perpendicular to axis (A): axis (B), (see Fig. 1).

2.3 Energy minimization

The expansion coefficients α_n's are treated as deformation parameters of the cluster. To minimize the total energy of the system, these parameters are optimized by the conjugate gradient method [24] under the constraints of volume conservation and a fixed distance, $D_{\rm cm}$, between the cluster and ion mass centers. Consequently, we obtain the total energy of the system as a function of $D_{\rm cm}$.

3 Results

We consider clusters Na_N^{Q+} which have a fissility $0.6 < X < 0.9$ ($X = (16\pi\sigma r_{\rm ws}^3)^{-1} Q^2/N$). The size N ranges arbitrarily from a hundred to a thousand.

Table 1. Systems that are treated in Figure 2.

System	Fissility X
$\mathrm{Na}_{1000}^{18+} + \mathrm{Na}_1^{1+}$	0.75
$\mathrm{Na}_{1050}^{19+} + \mathrm{Na}_1^{1+}$	0.80
$\mathrm{Na}_{1000}^{19+} + \mathrm{Na}_1^{1+}$	0.84
$\mathrm{Na}_{1000}^{20+} + \mathrm{Na}_1^{1+}$	0.93

The cluster shape is determined at each distance $D_{\rm cm}$ by optimizing the deformation parameters α_n's in equation (10) to minimize the total energy of the system. The number of deformation parameters is chosen to ensure the convergence of the total energy of the system. In practice, for axis (A), we take $n = 2, 3$ and 4 and for axis (B), $n = 2, 4, 6$ and 8 (due to the spatial symmetry, odd orders do not contribute).

In this section, we first describe the variation of the total energy with surface charge polarization and deformation. Next we show the shapes which minimize the total energy. Then we refer to the local fissility which measures the local competition between the Coulomb force and the surface tension at the surface of a cluster. Lastly we discuss the stability of charged clusters in presence of an external electric field.

3.1 Energy

In this subsection, we discuss the effects of surface charge polarization and deformation on the total energy of the system. As a typical example, we show in Figure 2 the total energy of the systems that are given in Table 1.

The clusters have about the same size ∼1000 but different values of fissility X. We consider the following four cases. In case 1, the cluster has a fixed spherical shape and no surface charge polarization is taken into account, *i.e.* the charges distribute uniformly on the surfaces. Case 1 thus corresponds to two point charges. In case 2, the cluster has still a fixed spherical shape but the polarization is now taken into account. In cases 3 and 4, the spherical shape constraint is relaxed; both the polarization and the cluster deformation are taken into account for axis (A) and axis (B) (cases 3 and 4, respectively).

The energies for cases 1 and 2 are calculated up to the touching distance of the spherical cluster and the ion (which is represented by the vertical dotted line in Fig. 2). Comparing case 2 with case 1, the decrease of the total energy due to charge polarization can be seen; the effect becomes larger as $D_{\rm cm}$ becomes smaller. At small $D_{\rm cm}$, one sees that there are energy barriers (maxima of the energy lines) for case 2. It means that the total Coulomb force acting on between the cluster and the ion changes from a repulsive one into an attractive one [12], as the result of the negative charge that is induced on the surface of the cluster facing the ion.

The polarization induced energy shift at the touching distance is about 1.5 eV and it does not change much for all systems listed in Table 1. Because the ion size is

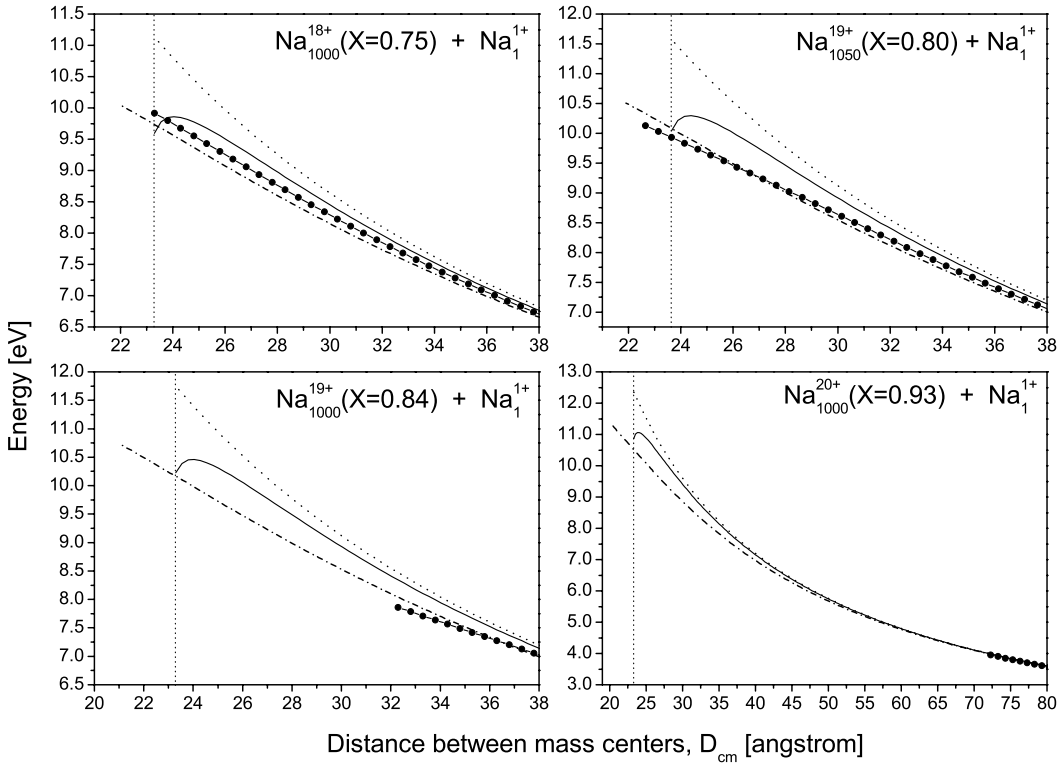

Fig. 2. Total energy as a function of distance, $D_{\rm cm}$, between mass centers of a cluster and an ion. The dotted line and the solid one are for spherical shapes without polarization (case 1) and with polarization (case 2), respectively. The dashed-dotted line and the solid one with circles are for cases 3 and 4 where both the polarization and the deformation are taken into account for axis (A) and axis (B), respectively. The vertical dotted line indicates the distance where the spherical cluster and the ion are touching. The origin of the energy is calibrated to the total energy of the system at infinite distance $D_{\rm cm}$.

small compared with the cluster size ($R_1 = 21.2$ Å for $N = 1000$ and $R_2 = 2.1$ Å), the contribution of the ion polarization to the total energy is very small. If the ion is a point charge, the variation of the total energy of the system due to polarization is determined by the cluster radius and the distance between the cluster and the point charge irrespective of the charge of the cluster. The same tendency is found even for smaller size clusters $N \sim 100$ ($R_1 \sim 10$ Å). The energy variations due to the polarization are almost the same (∼1.1 eV at the touching distance) irrespective of X.

Inclusion of the deformation of the cluster in addition to the polarization brings about a further variation of the total energy for cases 3 and 4. We start the calculation from a far distance $D_{\rm cm}$ with a spherical cluster as an initial shape, and optimize the cluster shape as mentioned above. We proceed the calculation toward the smaller $D_{\rm cm}$ (one step is 0.5 Å) with an initial shape of the cluster given by the optimum shape at the previous step.

As the ion approaches the cluster, the cluster deforms into an oblate shape for axis (A) and into a prolate shape for axis (B). The cluster develops a shape such that the surface facing the ion stays apart from the ion for both axis (A) and axis (B). Consequently, the polarization is smaller compared with that without the deformation at same $D_{\rm cm}$. As a result of deformation, the total energy of the system decreases from that without deformation. The deformation of the cluster and the variation of the total energy caused by the deformation become larger as $D_{\rm cm}$ becomes smaller.

At small $D_{\rm cm}$, a negative charge is induced on the surface of the cluster facing the ion as in case 2, but it is not large enough to cause an attractive force between the cluster and the ion. Therefore the total energy increases monotonously as $D_{\rm cm}$ decreases. In this study, we terminate the calculation when the cluster and the ion touch each other.

For $X = 0.75$, the energy for axis (A) is lower than that for axis (B). However, for a larger fissility $X = 0.80$, the energy for axis (B) is lower than that for axis (A) at small $D_{\rm cm}$ and a crucial difference appears between the cases for axis (A) and axis (B). For axis (A), a local minimum of the total energy is always found, whereas for axis (B), no local energy minima are found for $D_{\rm cm} < 22$ Å although the cluster and the ion are not touching yet. It means that the external electric field of the ion induces an instability of the cluster, even when the fissility of the latter is less than unity. The same instability also occurs for the clusters with $X = 0.84$ and $X = 0.93$ inside $D_{\rm cm} \sim 38$ Å and ∼71 Å, respectively.

Thus we infer that for axis (A), a local minimum of the total energy always exists irrespective of the cluster size, the charge and the distance $D_{\rm cm}$ as far as $X < 1$. At variance, for axis (B), the cluster becomes unstable in the

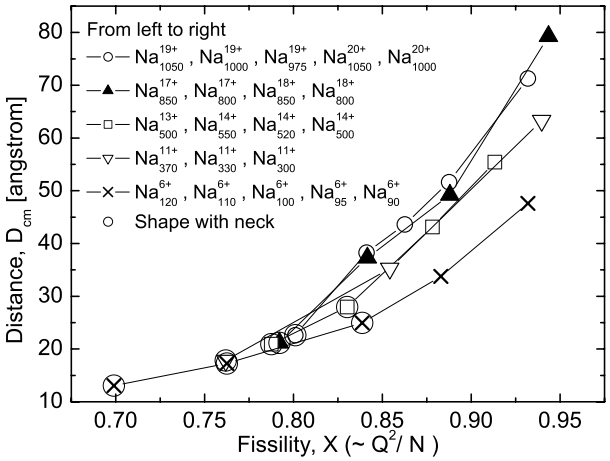

Fig. 3. Critical distance, $D_{\rm cm}^{\rm crit}$ against fissility, X. Similar sizes are connected with lines. Data with open circle means elongated shape with neck.

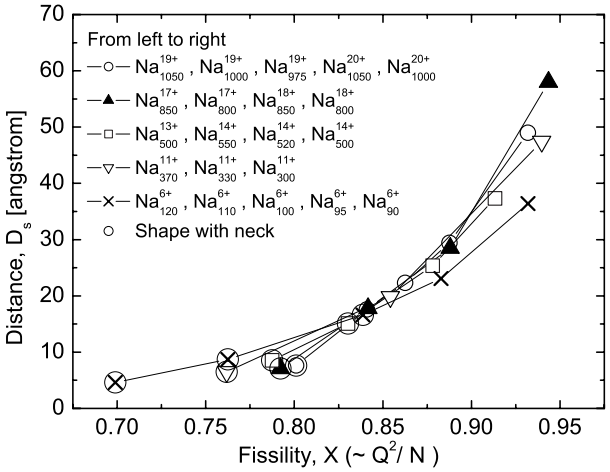

Fig. 4. Cluster-ion surface separation distance, $D_{\rm s}$ (along the line passing through the mass centers) against fissility, X.

external field of the ion, whenever the fissility of the cluster exceeds some limiting value and $D_{\rm cm}$ is smaller than some critical distance. We define the limiting value of the fissility as $X_{\rm limit}$, and define the critical distance as $D_{\rm cm}^{\rm crit}$. In Figure 3, we show the relation of the critical distance $D_{\rm cm}^{\rm crit}$ to the fissility X for various sizes N and charges Q. In this figure, the points which have about the same cluster size are connected with lines. Along each line, the smallest X expresses $X_{\rm limit}$ for this size. For instance, $X_{\rm limit}$ is 0.8 for $N \sim 1000$ and is 0.7 for $N \sim 100$. $D_{\rm cm}^{\rm crit}$ becomes larger as X increases. $D_{\rm cm}^{\rm crit}$ also increases as the size increases. It is found that the energy at $D_{\rm cm}^{\rm crit}$ for axis (B) is lower than that for axis (A) when the instability occurs.

In Figure 4, we also show the distance between the surfaces of the cluster and the ion (denoted as $D_{\rm s}$) for the same systems that are shown in Figure 3. The distance $D_{\rm s}$ is measured along the line passing through the mass centers of the cluster and the ion. In contrast to $D_{\rm cm}^{\rm crit}$, the surface distance $D_{\rm s}$ (at $D_{\rm cm}^{\rm crit}$) is approximately the same for the clusters with similar fissility X but with different

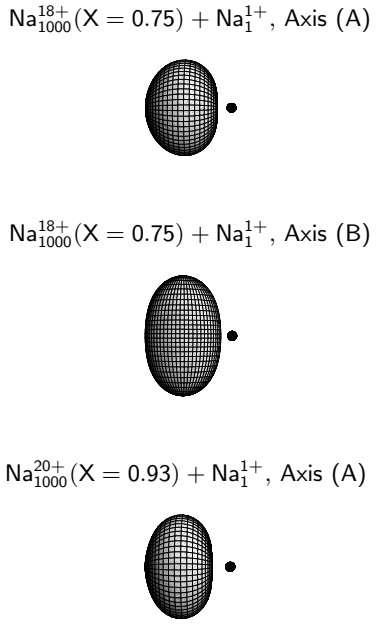

Fig. 5. Shapes of a cluster Na_{1000}^{Q+} in presence of an ion at touching distance, $D_{\rm cm} = 23.3$ Å. From the top, $X = 0.75$ for axis (A), $X = 0.75$ for axis (B) and $X = 0.93$ for axis (A).

size N, except for $N \sim 100$. This result suggests that the polarization at the surface facing the ion plays an important role in determining the stability of the cluster.

3.2 Cluster shape

In the top and the middle of Figure 5, we show the cluster shape for the system $\mathrm{Na}_{1000}^{18+}(X = 0.75) + \mathrm{Na}_1^{1+}$ at the distance $D_{\rm cm} = 23.3$ Å where the spherical cluster and the ion are touching, for axis (A) and axis (B), respectively. The clusters develop oblate shapes for axis (A) and prolate shapes for axis (B) in order to keep their surface away from the ion and to reduce the Coulomb energy. In the bottom of the figure, the system $\mathrm{Na}_{1000}^{20+}(X = 0.93) + \mathrm{Na}_1^{1+}$ at the same $D_{\rm cm}$ is shown for axis (A). Comparing the top with the bottom, one can see that the deformation becomes larger as the fissility increases, which is associated with a large variation of the total energy (see Fig. 2). From the top to the bottom of Figure 6, one sees the shape of the ($N \sim 1000$) cluster for axis (B) at $D_{\rm cm}^{\rm crit}$ for $X = 0.80$, 0.84 and 0.93, respectively.

In the absence of an external field, a charged droplet has a nearly spherical shape or a spheroidal shape at the saddle point of the potential energy when the fissility X is close to unity, and it has a dumbbell shape for lower fissilities, $X \leq 0.8$ [12,21]. If we suppose that this criterion also holds for a cluster in an external electric field, the cluster shape at the critical distance $D_{\rm cm}^{\rm crit}$ can be explained as follows. For $X = 0.93$, the cluster becomes unstable with a slight deformation from the spherical shape, so $D_{\rm cm}^{\rm crit}$ is relatively large. As X decreases, the cluster can deform more before the instability occurs, and $D_{\rm cm}^{\rm crit}$ becomes smaller. For $X = 0.80$, the cluster deforms enough to develop a

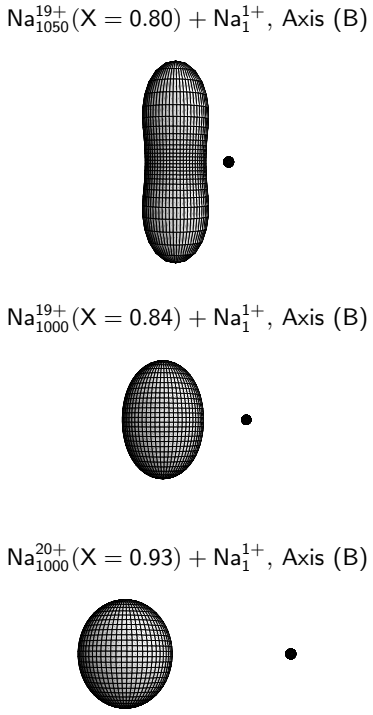

Fig. 6. Shapes of a cluster $\sim$ Na^{Q+}_{1000} in presence of an ion for axis (B), from the top, at $D^{\rm crit}_{\rm cm} = 22.6$ Å for $X = 0.80$, 38.3 Å for $X = 0.84$ and 71.3 Å for $X = 0.93$.

necked elongated shape, which might lead to fission (see the top of Fig. 6). However, for $X \leq 0.75$, the deformation stays small even when the ion comes very close to the cluster and the cluster does not go over the saddle point (see the middle of Fig. 5). Hence the cluster is stable at any distance $D_{\rm cm}$.

In Figures 3 and 4, the point with a circle means that the cluster has an elongated shape with a neck. It is seen that clusters with $X < 0.85$ are neck shaped.

3.3 Local fissility

In the presence of an ion induced electric field, a charged cluster with fissility $X > X_{\rm limit}$ becomes energetically unstable inside the distance $D^{\rm crit}_{\rm cm}$, for axis (B). Within the classical liquid drop model, the stability of a charged droplet is determined by the competition between the Coulomb energy and the surface energy. On the other hand, investigating directly the local competition between the Coulomb force and the surface tension at the surface of the droplet would be also of interest. In this subsection, we discuss the local stability at the cluster surface in terms of the competition between these forces at $D^{\rm crit}_{\rm cm}$.

We here define the Coulomb force per unit area $P_{\rm c}(\mathbf{r}_1)$ and the surface tension per unit area $P_{\rm s}(\mathbf{r}_1)$ at the surface of the cluster $\mathbf{r}_1$. For an ideal fluid, the direction of $P_{\rm s}$ is along the normal of the surface and is inward (in present case). $P_{\rm s}$ is given by the Laplace's formula in fluid mechanics:

$$P_{\rm s}(\mathbf{r}_1) = 2\sigma H(\mathbf{r}_1), \tag{12}$$

with the mean curvature $H(\mathbf{r}_1)$ given by the mean of the two principal curvatures at the surface point $\mathbf{r}_1$. The surface energy per unit area, σ, is assumed to be constant throughout the surface. At the surface of an ideal conductor, the direction of $P_{\rm c}$ is along the normal of the surface and its magnitude is equal to the energy density in the electric field. $P_{\rm c}(\mathbf{r}_1)$ is expressed as (in atomic units)

$$P_{\rm c}(\mathbf{r}_1) = \frac{1}{8\pi}\mathbf{E}(\mathbf{r}_1)^2 = 2\pi\rho(\mathbf{r}_1)^2, \tag{13}$$

where $\rho(\mathbf{r}_1)$ is the surface charge density, which is determined numerically in this work. $P_{\rm c}$ is always an outward force irrespective of the sign of the surface charge density.

Following Krappe's approach [22] who investigated the local stability at the tip of a charged spheroid by comparing $P_{\rm c}$ with $P_{\rm s}$ at the tip, we define a local fissility at each point $\mathbf{r}_1$ on the surface

$$X_{\rm local}(\mathbf{r}_1) \equiv \frac{P_{\rm c}(\mathbf{r}_1)}{P_{\rm s}(\mathbf{r}_1)}. \tag{14}$$

At infinite $D_{\rm cm}$, the cluster has a spherical shape for $X < 1$ and both $P_{\rm s}(\mathbf{r}_1)$ and $P_{\rm c}(\mathbf{r}_1)$ are constant; we denote them as $P^0_{\rm s}$ and $P^0_{\rm c}$, respectively. In that case, $X_{\rm local}(\mathbf{r}_1)$ is constant all over the surface of the cluster and coincides with X as one expects. As $D_{\rm cm}$ decreases and then the polarization and the deformation come in, $X_{\rm local}(\mathbf{r}_1)$ takes different values from place to place.

For the system $Na^{20+}_{1000}(X = 0.93) + Na^{1+}_{1}$, we show $X_{\rm local}$ for axis (B) at $D^{\rm crit}_{\rm cm} = 72.3$ Å in the middle of Figure 7. We represent the position on the cluster surface in spherical coordinates with the polar angle θ and the azimuthal angle ϕ as shown in the top of Figure 7. In the present numerical calculation, there are some area near the poles ($\theta \sim 0, \pi$) where we cannot evaluate $P_{\rm c}$ accurately. The polar axis is taken to be perpendicular to the line passing through the mass centers of the cluster and the ion, and to the geometrical symmetry axis of the cluster, to evaluate $P_{\rm c}$ accurately at the tips of the cluster that we are interested in.

$X_{\rm local}$ is larger at the surface opposite to the ion than at the surface facing the ion, because of the distribution of $P_{\rm c}$. In the bottom of Figure 7, $P_{\rm c}$ (normalized by $P^0_{\rm c}$) of the cluster for the same system is shown. The magnitude of $P_{\rm c}$ reflects the charge density *via* equation (13). Due to the presence of the positive charge of the ion, the positive charge of the cluster is slightly biased toward the surface opposite to the ion, on the whole. In particular, at the surface facing the ion (marked by the white cross in the figure), the positive charge density is the smallest and hence $X_{\rm local}$ is the smallest. $P_{\rm c}$ is the largest at the tips because the charge density becomes large. But $P_{\rm s}$ (proportional to the mean curvature H) is also the largest at the tip and becomes smaller toward the equator. Hence $X_{\rm local}$ is the largest at a place opposite to the ion but close to a tip.

If $X_{\rm local}(\mathbf{r}_1)$ becomes larger than unity at some $\mathbf{r}_1$, it means that the Coulomb force surpasses the surface tension, so that the cluster will be locally unstable at this place. In such a case, a protrusion might develop from the

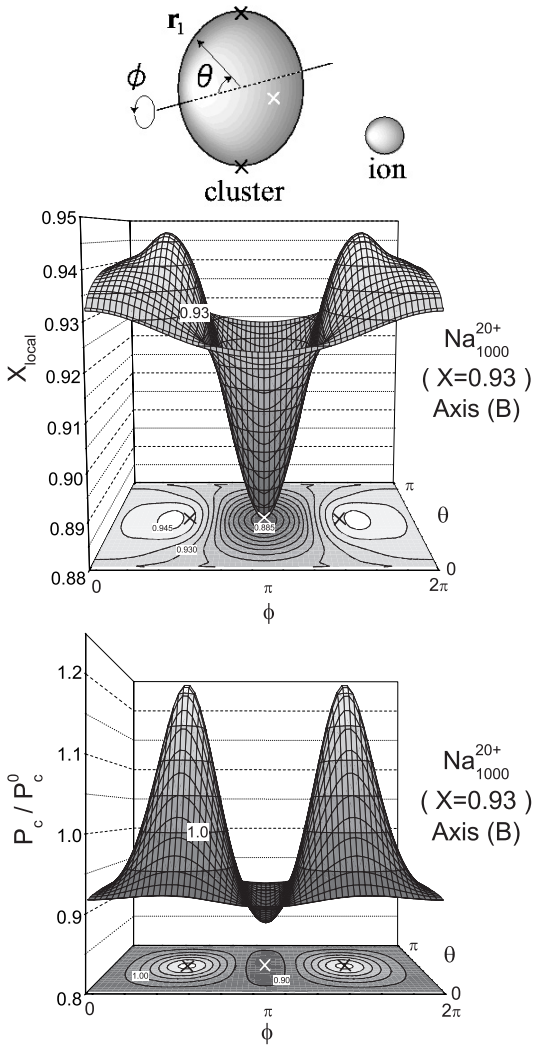

Fig. 7. Local fissility, $X_{\rm local}$ and $P_{\rm c}$ (normalized by $P_{\rm c}^0$) of a cluster are shown in the middle and the bottom, respectively. The polar axis, the polar angle θ and the azimuthal angle ϕ are shown in the top. A white cross at $\theta = \pi/2, \phi = \pi$ indicates the point facing the ion where the line passing through the mass centers intersects the cluster surface. Two black crosses at $\theta = \pi/2, \phi = \pi/2$ and $\theta = \pi/2, \phi = 3\pi/2$ locate the two tips of the prolate shape for axis (B). Data near the poles $\theta \sim 0, \pi$ where our calculations are inaccurate is not shown.

surface of the cluster and a small (positively) charged particle might be emitted. In the actual calculation, the deviation $|X_{\rm local} - X|$ becomes larger as $D_{\rm cm}$ becomes smaller. However, $X_{\rm local}$ is always found to be less than unity, even when $D_{\rm cm}$ reaches $D_{\rm cm}^{\rm crit}$.

3.4 Stability of clusters

In this subsection, we discuss the force that is effectively acting on the surface of a charged cluster. Without an external field, a droplet which has a fissility $X < 1$ is stable with respect to spherical shape. In order to balance the force which corresponds to the difference between $P_{\rm s}^0$ and $P_{\rm c}^0$, there must be a pressure of the liquid:

$$P_{\rm LD}^0 = P_{\rm s}^0 - P_{\rm c}^0 \ > 0. \tag{15}$$

In an external field, due to surface charge polarization and deformation, the forces effectively acting on at the surface of the cluster do not vanish. In that case, $P_{\rm s}(\mathbf{r}_1) - P_{\rm c}(\mathbf{r}_1)$ takes different values from place to place and we can generalize equation (15) as

$$P_{\rm LD} = \frac{\displaystyle\int_{S_1} (P_{\rm s} - P_{\rm c}) {\rm d}S_1}{\displaystyle\int_{S_1} {\rm d}S_1}, \tag{16}$$

which is constant all over the cluster, knowing that the pressure of a liquid is constant and directs outward along the normal of the surface.

We define the effective force per unit area as the sum of the forces acting on at the surface as

$$P_{\rm eff}(\mathbf{r}_1) \equiv P_{\rm LD} - P_{\rm s}(\mathbf{r}_1) + P_{\rm c}(\mathbf{r}_1). \tag{17}$$

The direction of $P_{\rm eff}$ is also along the normal of the surface $\hat{n}$. Here, the outward direction from the surface is set to be the positive one. From the definition of $P_{\rm LD}$, the integral of $P_{\rm eff}$ all over the surface vanishes as in the case of a spherical cluster without an external field. The total force acting on the cluster surface, *i.e.* the integration of $P_{\rm eff}\,\hat{n}$ as a vector all over the surface has to coincide with the total interaction Coulomb force between the cluster and the ion.

In Figure 8, for the system $\mathrm{Na}_{1000}^{20+}(X = 0.93) + \mathrm{Na}_1^{1+}$ at $D_{\rm cm}^{\rm crit}$, we show $P_{\rm eff}$ (normalized by $P_{\rm s}^0$) for the three types of deformation of the cluster: axis (B), the spherical shape and axis (A), respectively.

$P_{\rm eff}$ is negative (inward force) at the surface facing the ion where the positive charge density decreases; here, $P_{\rm s}$ is larger than the sum of $P_{\rm c}$ and $P_{\rm LD}$. On the other hand, $P_{\rm eff}$ is positive (outward force) at the opposite surface where $P_{\rm s}$ is smaller than the sum of $P_{\rm c}$ and $P_{\rm LD}$ (but still $P_{\rm s} - P_{\rm c} > 0$, see Fig. 7). Along the line that separates the points at the surface facing the ion from those opposite to it, $P_{\rm eff}$ almost vanishes for all deformations. That is, on both the surfaces that faces the ion and that is opposite to it, $P_{\rm eff}$ acts to push the surfaces away from the ion.

In order to shed light on the relation between $P_{\rm eff}$ and the stability of the cluster, we evaluate the inward force and the outward force as regard to X, N and the symmetry axis. As a rough estimate, we consider the maximum magnitude of the inward force (denoted by $P_{\rm eff}^{\rm near}$) and that of the outward force (denoted by $P_{\rm eff}^{\rm far}$).

In Figures 9 and 10, we show $P_{\rm eff}^{\rm near}$ and $P_{\rm eff}^{\rm far}$ for axis (B) and axis (A), respectively, for the same systems as in Figures 3 and 4 (at $D_{\rm cm}^{\rm crit}$). These pressures are normalized by $P_{\rm s}^0$ and the outward direction is the positive one (the data in the figures is restricted to shapes without neck). We also show the difference between $P_{\rm eff}^{\rm near}$ and $P_{\rm eff}^{\rm far}$ (denoted by $P_{\rm eff}^{\rm diff}$) which is the sum of $P_{\rm eff}^{\rm near}$ and $P_{\rm eff}^{\rm far}$ (*i.e.* the difference between the vectors, $P_{\rm eff}^{\rm near}\hat{n}_{\rm near} - P_{\rm eff}^{\rm far}\hat{n}_{\rm far}$)

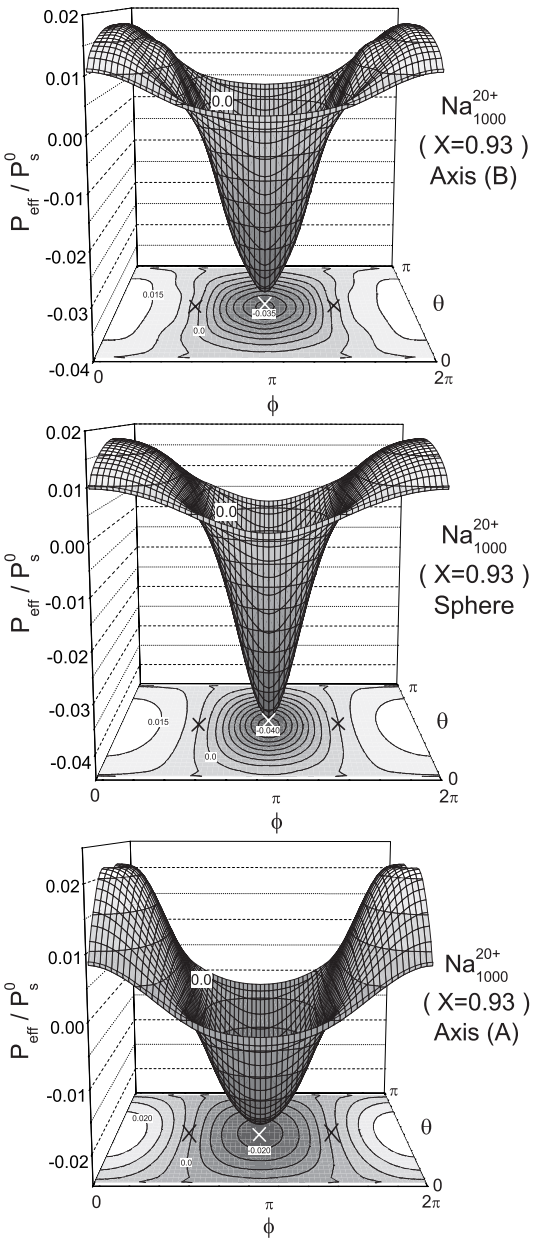

Fig. 8. $P_{\rm eff}$ (normalized by $P_{\rm s}^0$) of a cluster for three deformations: axis (B), spherical shape, and axis (A) from the top to the bottom, respectively. The coordinates system is the same as in Figure 7: the white cross is at $\theta = \pi/2, \phi = \pi$, and the two black crosses is at $\theta = \pi/2, \phi = \pi/2$ and $\theta = \pi/2, \phi = 3\pi/2$. The two black crosses indicate the tips of the prolate shape for axis (B), only.

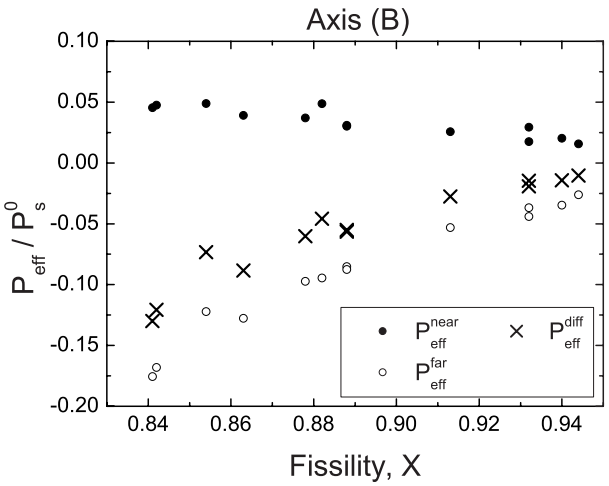

Fig. 9. $P_{\rm eff}^{\rm near}$, $P_{\rm eff}^{\rm far}$ and $P_{\rm eff}^{\rm diff}$ (including its sign and normalized by $P_{\rm s}^0$), for axis (B).

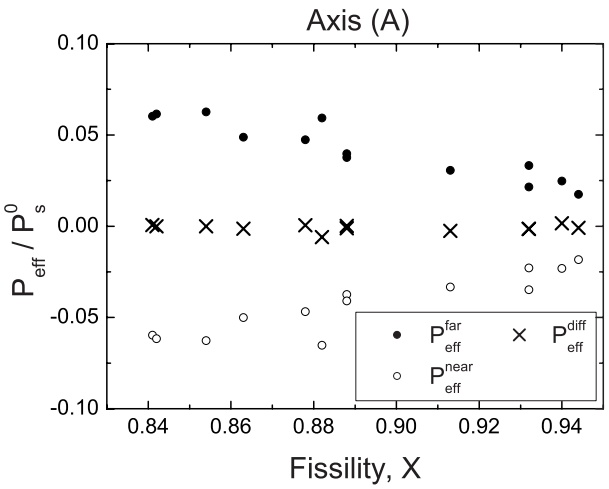

Fig. 10. $P_{\rm eff}^{\rm near}$, $P_{\rm eff}^{\rm far}$ and $P_{\rm eff}^{\rm diff}$ (including its sign and normalized by $P_{\rm s}^0$), for axis (A).

to express the balance between the force acting on the surface facing the ion and that opposite to the ion.

Neglecting small fluctuations of the data, $P_{\rm eff}^{\rm near}$, $P_{\rm eff}^{\rm far}$ and $P_{\rm eff}^{\rm diff}$ are determined essentially by X and are independent of the size of the cluster. For axis (A), the magnitudes of $P_{\rm eff}^{\rm near}$ and $P_{\rm eff}^{\rm far}$ increase slowly as X decreases, but $P_{\rm eff}^{\rm diff}$ almost vanishes. For axis (B), as X decreases, the magnitude of $P_{\rm eff}^{\rm near}$ becomes larger, while that of $P_{\rm eff}^{\rm far}$ does not change as much as $P_{\rm eff}^{\rm near}$. Thus, $P_{\rm eff}^{\rm diff}$ takes negative value and the magnitude becomes larger as X decreases.

The negative value of $P_{\rm eff}^{\rm diff}$ means that the cluster is pressed by the difference between $P_{\rm eff}^{\rm near}$ and $P_{\rm eff}^{\rm far}$ along the line passing through the mass centers of the cluster and the ion. If we set the cluster shape to be spherical at $D_{\rm cm}^{\rm crit}$, $P_{\rm eff}^{\rm diff}$ is again negative and the magnitude is larger than that for axis (B). The cluster should deform, in order to relax the pressure caused by the difference between $P_{\rm eff}^{\rm near}$ and $P_{\rm eff}^{\rm far}$, from a spherical shape into an oblate shape for axis (A) and into a prolate shape for axis (B), respectively, which is accordance with our results shown in Figures 5 and 6. For instance, the system in Figure 8, $P_{\rm eff}^{\rm diff}/P_{\rm s}^0$ are about 0.001, -0.019 and -0.026 for axis (A), axis (B) and spherical shape, respectively.

As for the stability, for axis (A), $P_{\rm eff}^{\rm diff}$ stays almost constant and close to zero. Hence the cluster is stable. On the other hand, $P_{\rm eff}^{\rm diff}$ does not vanish for axis (B). Intuitively, the cluster is pressed and becomes unstable inside $D_{\rm cm}^{\rm crit}$

where it passes over the saddle of the potential energy barrier; the cluster is *not* stretched by P_c at the tip. As $P_{\rm eff}^{\rm diff}$ becomes larger with decreasing X, the cluster is further pressed and deforms largely. Since $P_{\rm eff}^{\rm diff}$ is determined by X, we expect that $P_{\rm eff}^{\rm diff}$ has an important role in determining the shape of the cluster. Actually, the shapes of the clusters with same extent of X at $D_{\rm cm}^{\rm crit}$ are very similar.

Let us consider the origin of the difference in $P_{\rm eff}$ among the different shapes for axis (A), axis (B) and the spherical shape. $P_{\rm eff}^{\rm far}$ takes the almost same value for the three different types of deformations. Hence $P_{\rm eff}^{\rm diff}$ reflects the difference of $P_{\rm eff}^{\rm near}$. In addition to the result in Figure 4, this result also suggests us that the polarization at the surface facing the ion significantly affects the deformation and the stability of the cluster.

4 Summary

In the present work, we have investigated the stability of highly charged metal clusters (with fissility $X < 1$) in the external electric field of an ion within the classical liquid drop model, taking account of surface charge polarization and deformation. We see that the effect of the cluster deformation on the total energy of the system is as important as that of the polarization. As the ion approaches, the deformation of the cluster becomes larger. The deformation is larger for the cluster with larger fissility, if the distance between the mass centers of the cluster and the ion $D_{\rm cm}$ is the same.

As for the deformation of the cluster, we consider the two types of symmetry axis, *i.e.* axis (A) and axis (B) (see Fig. 1). The cluster deforms into an oblate shape for axis (A) and into a prolate shape for axis (B).

As an ion approaches, in the situation axis (B), a charged cluster with $X > X_{\rm limit}$ becomes energetically unstable inside $D_{\rm cm}^{\rm crit}$. When the instability occurs, the total energy of the system for axis (B) is lower than that for axis (A) at $D_{\rm cm}^{\rm crit}$. $X_{\rm limit}$ ranges from 0.7 to 0.8, depending on the size of the cluster. The value of $D_{\rm cm}^{\rm crit}$ depends on X and the size of the cluster, but its surface distance between the cluster and the ion $D_{\rm s}$ is approximately determined solely by X.

Investigating the effective force $P_{\rm eff}$ acting on the surface of the cluster at $D_{\rm cm}^{\rm crit}$, we see that the stability and deformation of a cluster significantly relate to the polarization of the surface charge due to the external electric field of the ion. The (positive) charge density at the surface facing the ion decreases and that at the surface opposite to the ion increases. Consequently, $P_{\rm eff}$ directs inward at the surface facing the ion and outward at the surface opposite to the ion.

We find that the stability of the cluster and its possible deformation are roughly estimated by the difference $P_{\rm eff}^{\rm diff}$ between the maximum magnitude of the inward force $P_{\rm eff}^{\rm near}$ and that of the outward force $P_{\rm eff}^{\rm far}$. Those quantities ($P_{\rm eff}^{\rm near}$, $P_{\rm eff}^{\rm far}$ and $P_{\rm eff}^{\rm diff}$) are essentially determined by X and is not sensitive to the size of the cluster. $P_{\rm eff}^{\rm diff}$ for the spherical shape at $D_{\rm cm}^{\rm crit}$ is larger than that for axis (B); the cluster deforms in order to relax $P_{\rm eff}^{\rm diff}$. For axis (B), $P_{\rm eff}^{\rm diff}$ does not vanish and less than zero, which means that the cluster is pressed by the difference between $P_{\rm eff}^{\rm near}$ and $P_{\rm eff}^{\rm far}$ and becomes unstable inside $D_{\rm cm}^{\rm crit}$. On the other hand, at the same distance $D_{\rm cm}^{\rm crit}$, $P_{\rm eff}^{\rm diff}$ almost vanishes for axis (A) and the cluster is stable against this deformation.

We find that in the external electric field of the ion, the cluster can become unstable even when the fissility X is less than unity. Surface charge polarization has the main contribution to the instability. Here, we see a characteristic difference between metal clusters and atomic nuclei. For atomic nuclei, the charge cannot be polarized because the distribution of the protons firmly connects to that of the neutrons. Hence, the instability caused by an external electric field is a special feature of metal clusters. However, since we use only a few deformation parameters to express the shape of the cluster, we cannot describe in detail how the cluster collapses.

In this study, we use the classical liquid model. In nuclear physics, the quantum effect of protons and neutrons closely relates to the deformation of the atomic nuclei and its stability. For more detailed discussion, it would be desirable to treat the quantal behavior of the valence electrons.

For actual reactions, the dynamics plays an important role. Since we calculate the static potential energy, our treatment is easily applied to the case such that the time scale for the ion to stay close to the cluster $t_{\rm ion}$ is comparable with that for the cluster to deform $t_{\rm cluster}(\sim 10^{-12})$. For other case, the instability is expected to occur with the probability $\sim t_{\rm ion}/t_{\rm cluster}$.

The authors would like to express their gratitude to Professor Yasuhisa Abe, Yukawa Institute for Theoretical Physics, Kyoto University, Japan for the discussion in the early stage of this work. The authors also would like to thank Professor Masahisa Ohta, Konan University, Japan for his encouragement. C.G. warmly acknowledges the hospitality and support of the Yukawa Institute for Theoretical Physics.

References

1. C. Bréchignac *et al.*, Z. Phys. D **19**, 1 (1991); Phys. Rev. B **44**, 11386 (1991)
2. T.P. Martin *et al.*, Chem. Phys. Lett. **196**, 113 (1992); Z. Phys. D **31**, 191 (1994)
3. C. Bréchignac *et al.*, Phys. Rev. Lett. **72**, 1636 (1994)
4. C. Bréchignac *et al.*, Phys. Rev. Lett. **77**, 251 (1996)
5. C. Bréchignac *et al.*, Phys. Rev. Lett. **81**, 4612 (1998)
6. M. Heinebrodt *et al.*, Z. Phys. D **40**, 334 (1997); Eur. Phys. J. D **9**, 133 (1999)
7. F. Chandezon *et al.*, Phys. Rev. Lett. **74**, 3784 (1995); Phys. Rev. A **63**, 051201(R) (2001)
8. C. Guet, B.A. Huber, S.A. Blundell, Nucl. Instrum. Meth. B **107**, 36 (1996)
9. C. Guet *et al.*, Z. Phys. D **40**, 317 (1997)
10. T. Bergen *et al.*, AIP Conf. Proc. **416**, 148 (1998)

11. F. Chandezon *et al.*, Phys. Rev. Lett. **87**, 153402 (2001)
12. U. Näher, S. Bjørnholm, S. Frauendorf, F. Garcias, C. Guet, Phys. Rep. **285**, 245 (1997)
13. R.N. Barnett *et al.*, J. Chem. Phys. **94**, 608 (1991); Phys. Rev. Lett. **67**, 3058 (1991)
14. O. Schapiro *et al.*, Z. Phys. D **41**, 219 (1997)
15. Y. Li, E. Blaisten-Barojas, D.A. Papaconstantopoulos, Chem. Phys. Lett. **268**, 331 (1997); Phys. Rev. B **57**, 15519 (1998)
16. F. Calvayrac, P.-G. Reinhard, E. Suraud, J. Phys. B **31**, 5023 (1998); Eur. Phys. J. D **9**, 389 (1999)
17. P. Blaise, S.S. Blundell, C. Guet, R. Zope, Phys. Rev. Lett. **87**, 063401 (2001)
18. N. Bohr, J.A. Wheeler, Phys. Rev. **56**, 426 (1939)
19. O. Hahn, F. Straussmann, Naturwissenschaften **27**, 11 (1939)
20. Lord Rayleigh, Phil. Mag. **14**, 185 (1882)
21. V.V. Pashkevich, H.J. Krappe, J. Wehner, Z. Phys. D **40**, 338 (1997)
22. H.J. Krappe (unpublished)
23. H. Koizumi, S. Sugano, Y. Ishii, Z. Phys. D **28**, 223 (1993)
24. W.H. Press, B.P. Flannery, S.A. Teukolsky, W.T. Vetterling, *Numerical Recipes* (Cambridge University Press, 1990)